

Published in final edited form as:

Bioorg Med Chem Lett. 2013 May 15; 23(10): 2996–3000. doi:10.1016/j.bmcl.2013.03.032.

Discovery of ML326: the first sub-micromolar, selective M₅ PAM

Patirck R. Gentry^{b,c,d}, Thomas M. Bridges^{b,c}, Atin Lamasal^e, Paige N. Vinson^{b,c}, Emery Smith^e, Peter Chase^e, Peter S. Hodder^{e,f}, Julie L. Engers^{b,c}, Colleen M. Niswender^{a,b,c}, J. Scott Daniels^{a,b,c}, P. Jeffrey Conn^{a,b,c}, Michael R. Wood^{a,b,c,d}, and Craig W. Lindsley^{a,b,c,d,*}

^aDepartment of Pharmacology, Vanderbilt University Medical Center, Nashville, TN 37232, USA

^bVanderbilt Center for Neuroscience Drug Discovery, Vanderbilt University Medical Center, Nashville, TN 37232, USA

^cVanderbilt Specialized Chemistry Center for Probe Development (MLPCN), Nashville, TN 37232, USA

^dDepartment of Chemistry, Vanderbilt University, Nashville, TN 37232, USA

^eScripps Research Institute Molecular Screening Center, Lead Identification Division, Translational Research Institute, 130 Scripps Way, Jupiter, FL 33458, USA

^fDepartment of Molecular Therapeutics, Scripps Florida, 130 Scripps Way, Jupiter, FL 33458, United States

Abstract

This letter describes the further chemical optimization of the M₅ PAM MLPCN probes ML129 and ML172. A multi-dimensional iterative parallel synthesis effort quickly explored isatin replacements and a number of southern heterobiaryl variations with no improvement over ML129 and ML172. An HTS campaign identified several weak M₅ PAMs (M₅ EC₅₀ >10 μM) with a structurally related isatin core that possessed a southern phenethyl ether linkage. While SAR within the HTS series was very shallow and unable to be optimized, grafting the phenethyl ether linkage onto the ML129/ML172 cores led to the first sub-micromolar M₅ PAM, ML326 (VU0467903), (human and rat M₅ EC₅₀s of 409 nM and 480 nM, respectively) with excellent mAChR selectivity (M₁-M₄ EC₅₀s <30 μM) and a robust 20-fold leftward shift of the ACh CRC.

Keywords

Muscarinic acetylcholine receptors; M₅; Positive allosteric modulator (PAM); ML326

There are five muscarinic acetylcholine receptor (mAChR) subtypes (M₁ – M₅) widely expressed in both the central nervous system (CNS) and periphery of mammals.^{1–5} These receptors, whose endogenous agonist is acetylcholine (ACh), play critical roles in regulating a variety of diverse physiological processes. Within the CNS, the M₁, M₄ and M₅ subtypes are believed to be the most important with respect to normal neuronal functioning.^{1–5} Of these three, M₅ is the least studied as a combined result of its lower expression levels⁶ (< 2% of total muscarinic receptor population within the brain) and, until recently, a near absence

© 2013 Elsevier Ltd. All rights reserved

*To whom correspondence should be addressed: craig.lindsley@vanderbilt.edu.

Publisher's Disclaimer: This is a PDF file of an unedited manuscript that has been accepted for publication. As a service to our customers we are providing this early version of the manuscript. The manuscript will undergo copyediting, typesetting, and review of the resulting proof before it is published in its final citable form. Please note that during the production process errors may be discovered which could affect the content, and all legal disclaimers that apply to the journal pertain.

of highly selective M₅ receptor ligands. Much of our current understanding surrounding the function of M₅ has come from M₅ receptor localization, M₅ knock-out mice⁷ and experiments conducted with non-selective muscarinic ligands.⁸ It is intriguing to note that the M₅ receptor is the only muscarinic receptor observed in the substantia nigra pars compacta (based on mRNA detection),^{9,10} leading to the prediction that M₅ functions in addiction/reward mechanisms. This hypothesis was supported in man through the clinically observed correlation between a specific M₅ gene mutation and an increase in cigarette consumption (+27%), as well as, an increased risk for cannabis dependence (+290%).¹¹ Additionally, M₅ receptors have been localized on the cerebrovascular system and shown to be critical in the ACh-induced dilation necessary for normal blood perfusion.¹² In a broader sense, M₅ KO mice show decreased prepulse inhibition,¹³ CNS neuronal abnormalities and cognitive deficits,¹⁴ thus supporting the potential for M₅ ligands in the treatment of numerous CNS disorders including schizophrenia, Alzheimer's disease, ischemia and migraine.¹⁻⁵

To date, few M₅ PAMs have been reported,¹⁵⁻¹⁷ and none of these display the potency and efficacy necessary to definitively probe the role of selective M₅ activation (Fig. 1); therefore, in this Letter, we detail the further optimization of these ligand, and the discovery of the first submicromolar and selective M₅ PAMs.

Within the isatin scaffold, alternate substitution afforded a highly selective M₁ PAM, ML137, **4**.¹⁸ We recently reported on a number of replacements (tertiary hydroxyls and spirocyclic replacements, etc.) for the isatin moiety that maintained M₁ PAM activity (Fig. 2).^{19,20} Therefore, our optimization plan for ML129 consisted of evaluating both spirocyclic and other replacements for the isatin moiety, while continuing to investigate alternatives for the southern *p*-OMe benzyl motif in an effort to improve M₅ PAM potency to below 1 μM (Fig. 3).

First, we explored alternatives to the 5-OCF₃ moiety on the isatin core, and despite evaluating other positions and alternate functionalities, all were devoid of M₅ PAM activity. Employing the chemistry previously reported for analogs **5** of ML137,¹⁹ we prepared the corresponding 3° hydroxyl and dioxalane analogs of ML129, and while there was a slight elevation in the ACh max, all of the analogs were >10 μM as M₅ PAMs, indicating a disconnect in the SAR between M₁ and M₅. We next explored novel 3° hydroxyl analogs with diverse functionalities, which proved to be more productive. Treatment of ML129 with DABCO in nitromethane afforded the 3° alcohol **7** in quantitative yield (Scheme 1);²¹ importantly, **7** was of comparable potency and efficacy to ML129 (M₅ EC₅₀ = 1.4 μM, 75% ACh Max), but the nitro moiety was not attractive as an *in vivo* probe.

This led us to explore other 3° alcohols possessing heterocycles, and most notably pyridines. Here, we employed two routes to survey pyridyl analogs **8** and pyridyl methyl homologs **11** (Scheme 2). Again, utilizing ML129 as starting material, exposure to a functionalized pyridyl boronic acid **9** under Cu(OTf)₂ catalysis, affords analogs **8** in 25–70% yields.²² We also employed direct lithiation/addition in some instances.²³ The homologated congeners **11** were easily accessed following the Li protocol,²⁴ employing picolines under Bronsted acid catalysis. SAR again proved shallow, with all analogs **11** showing no activity as M₅ PAMs; however, one of the 3-pyridyl-based 3° hydroxyls **8a** proved to be a moderately active M₅ PAM (M₅ EC₅₀ = 2.2 μM, 74% ACh Max), but SAR was steep.³

We therefore elected to introduce a more subtle variant of the isatin carbonyl in the form of a spiro-oxetane, and evaluate this carbonyl isostere for M₅ activity (Scheme 3). A Wittig reaction with ML129 provided **12**, which was smoothly converted into the diol **13** in 57% overall yield. Mono-triflation of **13** and nucleophilic displacement proceeded in low yield

(~6%) to the spiroxetane **14**.²⁵ Interestingly, **14** was inactive as an M₅ PAM, and only afforded a marginal base-line increase in the ACh Max.

Other modifications, such as spiro-pyrrolidines and dioxalanes, which were well tolerated for M₁ PAM activity in the ML137 series,^{19,20} were uniformly inactive on the ML129 scaffold. Clearly, SAR was steep and did not cross-over between M₁ and M₅. Moreover, despite the synthesis and screening of hundreds of analogs of ML129, surveying multiple regions, we were unable to develop a submicromolar M₅ PAM.

At this point, we pursued a new high throughput screen (HTS) for M₅ run in triple-add mode performed on the MLPCN screening deck (~360,000 compounds, PubChem AID 624103). Early in the process, and prior to official 'hit' confirmation (Fig. 4), we noticed a structurally related, weak single-point (31% @ 3 μM) hit, CID2145491 (**15**). This 'hit' possessed a phenethyl ether linkage, a moiety we had not yet explored on the ML129 core, and we were very surprised to find an isatin core without the 5-OCF₃ moiety, and a 7-methyl group¹⁵ with activity at M₅. We then reviewed the preliminary HTS data, and found a number of related compounds **16** with diverse functionality on the phenyl ring of the phenethyl ether, as well as either a 5- or 7-methyl group on the isatin core with weak M₅ activity (23–60% ACh max at 30 μM). Based on these data, we immediately questioned if the juxtaposition of ML129 with **15**, leading to analog **17** would lead to an improved M₅ PAM.

To evaluate this possibility, we prepared **17** by alkylating the 5-OCF₃ isatin **18** with commercial (2-bromoethoxy)benzene under microwave-assisted conditions in 82% yield (Scheme 4).²⁶

Gratifyingly, this structural modification led to one of the most potent M₅ PAM we have ever identified. **17** (VU0467903), later declared an MLPCN probe and given the designation ML326, was a potent M₅ PAM (Fig. 5) on both human (EC₅₀ = 409 nM, 91% ACh Max, pEC₅₀ = 6.39±0.04) and rat M₅ (EC₅₀ = 500 nM, 59% ACh Max). In fold-shift assays, ML326 afforded a robust 20-fold leftward shift of the ACh CRC, and was found to highly selective versus M₁-M₄ (EC₅₀s >30 μM). Very encouraged by the initial *in vitro* potency and selectivity profile for ML326 we prepared gram quantities and set about characterizing it through our in-house tier 1 DMPK assays (PPB, rat/human microsomal stability with predicted intrinsic clearance, P₄₅₀ inhibition, rat brain homogenate binding, etc.) and single dose PK/CNS exposure in rat. Many of these experiments were initiated in parallel, including the collection of rat plasma/brain samples; however we encountered insurmountable LCMS/MS analytical quantization issues due to poor ionization of ML326 using ESI, APPI, and APCI ionization probes, which prevented the determination of routine tier 1 DMPK parameters and *in vivo* rat exposure. Alternative methods including chemical derivatization and UV absorbance also failed to provide the requisite sensitivity for detection of ML326 thus preventing the completion of numerous studies. However, we were able to assess that ML326 had relatively clean CYP and ancillary pharmacology profiles.

Based on this promising data, we prepared other analogs **19** (Table 1) with substituents in the phenyl ring of **17**, following the route depicted in scheme 4. While this afforded a number of potent and selective M₅ PAMs, they all suffered from the same poor ionization profiles which precluded extensive DMPK profiling. Based on the ionization issue and relatively flat SAR, this series is no longer the subject of chemical optimization.

In summary, further elaboration of the ML129 M₅ PAM structure has been explored, and SAR was particularly steep. Insight from a weak M₅ PAM HTS hit led to the hybridization with ML129 to afford ML326 (VU0467903), the first highly selective (>30 μM versus M₁-M₄) and sub-micromolar (human (EC₅₀ = 409 nM, 91% ACh Max) and rat M₅ (EC₅₀ = 500

nM, 59% ACh Max)) M₅ PAM. Interestingly, the preliminary HTS hits that inspired the structural modifications to ML129, leading to ML326 did not confirm upon re-order and full CRC. Finally, the poor ionization of ML326 precluded in-depth DMPK profiling; however, ML3276 is a valuable *in vitro* probe and is serving as an important probe in electrophysiology studies, which will be reported shortly.

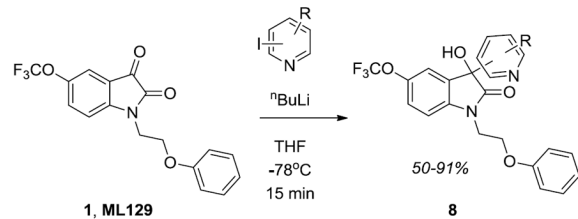
Acknowledgments

The authors thank the NIH (U54MH084659) and William K. Warren, Jr. who funded the William K. Warren, Jr. Chair in Medicine (to CWL). Vanderbilt University is a Specialized Chemistry Center within the MLPCN and all the ML# probes are freely available upon request. Scripps was supported by the National Institute of Health Molecular Library Probe Production Center grant U54 MH084512. We thank Lina DeLuca (Lead Identification Division, Scripps Florida) for compound management.

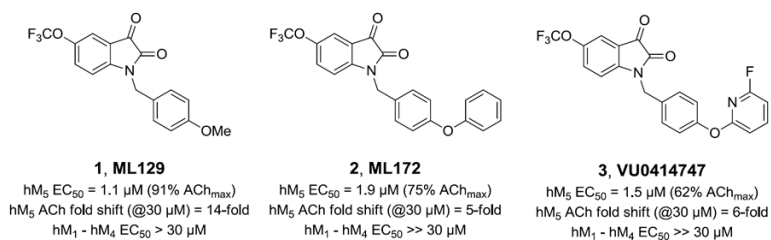
References

1. Bonner TI, Buckley NJ, Young AC, Brann MR. *Science*. 1987; 237:527–532. [PubMed: 3037705]
2. Dencker D, Thomsen M, Wörtwein G, Weikop P, Cui Y, Jeon J, Wess J, Fink-Jensen A. *ACS Chem. Neurosci.* 2012; 3:80–89. [PubMed: 22389751]
3. Melancon BJ, Hopkins CR, Wood MR, Emmitte KA, Niswender CM, Christopoulos A, Conn PJ, Lindsley CW. *J. Med. Chem.* 2012; 55:1445–1464. [PubMed: 22148748]
4. Bridges TM, LeBois EP, Hopkins CR, Wood MR, Jones JK, Conn PJ, Lindsley CW. *Drug News & Perspect.* 2010; 23:229–240.
5. Conn PJ, Jones C, Lindsley CW. *Trends in Pharm. Sci.* 2009; 30:148–156. [PubMed: 19201489]
6. Yasuda RP, Ciesla W, Flores LR, Wall SJ, Li M, Satkus SA, Weisstein JS, Spagnola BV, Wolfe BB. *Mol. Pharmacol.* 1993; 43:149–157. [PubMed: 8429821]
7. Wess J, Eglén RM, Gautam D. *Nat. Rev. Drug Discov.* 2007; 6:721–733. [PubMed: 17762886]
8. Steidl S, Miller AD, Blaha CD, Yeomans. *PLoS ONE*. 2011; 6(11):e27538. doi:10.1371/journal.pone.0027538. [PubMed: 22102904]
9. Vilaro MT, Palacios JM, Mengod G. *Neurosci. Lett.* 1990; 114:154–159. [PubMed: 2395528]
10. Weiner DM, Levey AI, Brann MR. *Proc. Natl. Acad. Sci. USA*. 1990; 87:7050–7054. [PubMed: 2402490]
11. Anney RJL, Lotfi-Miri M, Olsson CA, Reid SC, Hemphill SA, Patton GC. *BMC Genetics*. 2007; 8(46) doi:10.1186/1471-2156-8-46.
12. Yamada M, Lamping KG, Duttaroy A, Zhang W, Cui Y, Bymaster FP, McKinzie DL, Felder CC, Deng C-X, Faraci FM, Wess J. *Proc. Natl. Acad. Sci. USA*. 2001; 98:14096–14101. [PubMed: 11707605]
13. Thomsen M, Wörtwein G, Fink-Jessen A, Woldbye DPD, Wess J, Caine SB. *Psychopharmacology*. 2007; 192:97–110. [PubMed: 17310388]
14. Araya R, Noguchi T, Yuhki M, Kitamura N, Higuchi M, Saido TC, Seki K, Itohara S, Kawano M, Tanemura K, Takashima A, Yamada K, Kondoh Y, Kanno I, Wess J, Yamada M. *Neurobiol. Dis.* 2006; 24:334–344. [PubMed: 16956767]
15. Bridges TM, Marlo JE, Niswender CM, Jones CK, Jadhav SB, Gentry PR, Plumley HC, Weaver CD, Conn PJ, Lindsley CW. *J. Med. Chem.* 2009; 52:3445–3448. [PubMed: 19438238]
16. Bridges TM, Kennedy JP, Cho HP, Breining ML, Gentry PR, Hopkins CR, Conn PJ, Lindsley CW. *Bioorg. Med. Chem. Lett.* 2010; 20:558–562. [PubMed: 20004578]
17. Bridges TM, Kennedy JP, Hopkins CR, Conn PJ, Lindsley CW. *Bioorg. Med. Chem. Lett.* 2010; 20:5617–5622. [PubMed: 20801651]
18. Bridges TM, Kennedy JP, Cho HP, Conn PJ, Lindsley CW. *Bioorg. Med. Chem. Lett.* 2010; 20:1972–1975. [PubMed: 20156687]
19. Melancon BJ, Poslunsey MS, Gentry PR, Tarr JC, Mattmann ME, Bridges TM, Utley TJ, Sheffler DJ, Daniels JS, Niswender CM, Conn PJ, Lindsley CW, Wood MR. *Bioorg. Med. Chem. Lett.* 2013; 23:412–416. [PubMed: 23237839]

20. Poslunsey, MS.; Melancon, BJ.; Gentry, PR.; Bridges, TM.; Utley, TJ.; Sheffler, DJ.; Daniels, JS.; Niswender, CM.; Conn, PJ.; Lindsley, CW.; Wood, MR. *Bioorg. Med. Chem. Lett.* 2013. DOI: <http://dx.doi.org/10.1016/j.bmcl.2013.01.017>
21. Meshram HM, Ramesh P, Kumar S, Swetha A. *Tetrahedron Lett.* 2011; 52:5862–5864.
22. Zhang J, Chen J, Ding J, Liu M, Wu H. *Tetrahedron.* 2011; 67:9347–9351.
23. Scheme to access analogs **8** via lithiation/addition sequence.



24. Niu R, Xiao J, Liang T, Li X. *Org. Lett.* 2012; 14:676–679. [PubMed: 22273253]
25. Wuitschik G, Carreira EM, Wagner B, Fischer H, Parrilla I, Schuler F, Rogers-Evans M, Muller K. *J. Med. Chem.* 2010; 53:3227–3246. [PubMed: 20349959]
26. 1-(2-phenoxyethyl)-5-(trifluoromethoxy)indoline-2,3-dione, ML326: The title compound was synthesized in one step from commercially available starting materials according to the following procedure. Into a 20 mL microwave reaction vial, containing a magnetic stir bar, were weighed 5-(trifluoromethoxy)isatin (460 mg, 2.0 mmol), K_2CO_3 (550 mg, 4.0 mmol), KI (33 mg, 0.20 mmol), followed by acetonitrile (20 mL, 0.1 M) and 2-bromoethyl phenyl ether (480 mg, 2.4 mmol). After being sealed with a crimp cap, the vessel was placed in a microwave reactor and heated to 160 °C for 10 minutes, with magnetic stirring. After cooling to ambient temperature, the reaction was diluted with CH_2Cl_2 (~20 mL) and washed with brine. The organic layer was separated and dried over Na_2SO_4 . Solvent was removed under reduced pressure and the crude product was purified via flash column chromatography (silica gel, hexane/ethyl acetate, 0% to 50% ethyl acetate gradient). Product containing fractions were combined and the solvents removed under reduced pressure to obtain 583 mg of ML326 (83% yield) as a red-orange powder. TLC R_f = 0.79 (hexane/ethyl acetate 1:1); ^1H NMR (400 MHz, CDCl_3 calibrated to 7.26) δ 7.52–7.46 (m, 2H), 7.31–7.25 (m, 3H), 6.98 (t, J = 7.4 Hz, 1H), 6.82 (d, 2H), 4.28 (t, J = 5.0 Hz, 2H), 4.17 (t, J = 5.0 Hz, 2H); ^{13}C NMR (125 MHz, CDCl_3 calibrated to 77.16) δ 182.25, 158.27, 157.93, 150.01, 145.44, 131.02, 129.78, 121.75, 118.32, 114.39, 112.89, 65.94, 40.62; HRMS calcd for $\text{C}_{17}\text{H}_{13}\text{NO}_4\text{F}_3$ [M+H] $^+$; 352.0797 found 352.0795;.

**Figure 1.**

Structures and activities of the reported M_5 PAMs **1–3**. All three were derived from a *pan*- M_1 , M_3 , M_5 -PAM that afforded both M_1 selective PAMs and, by virtue of the 5-OCF₃ moiety, M_5 selective PAMs.

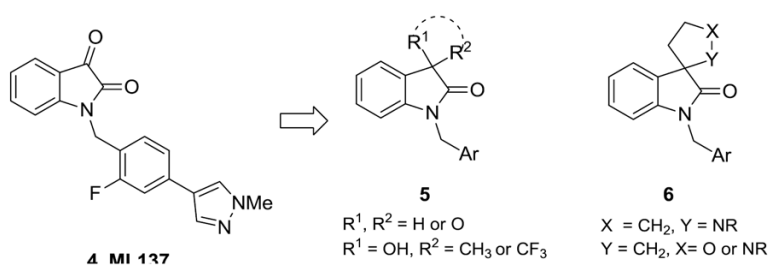


Figure 2. Structures and activities of the reported M_1 PAMs 4–6. Multiple productive replacements (tertiary hydroxyls, dioxalanes and spiro furans/pyrroles) were identified for the isatin moiety of ML137 that maintained selective M_1 PAM activity.

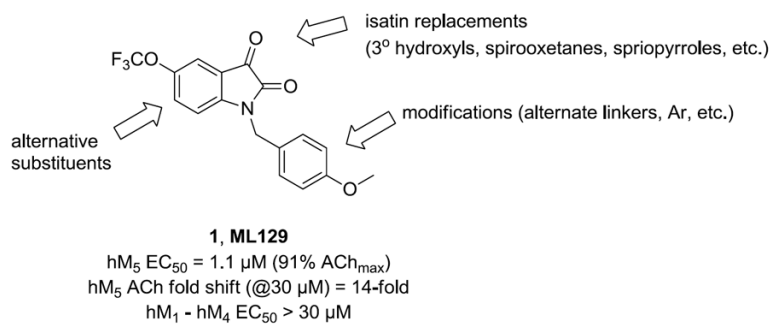


Figure 3.
Multi-dimensional chemical optimization plan for ML129 (**1**).

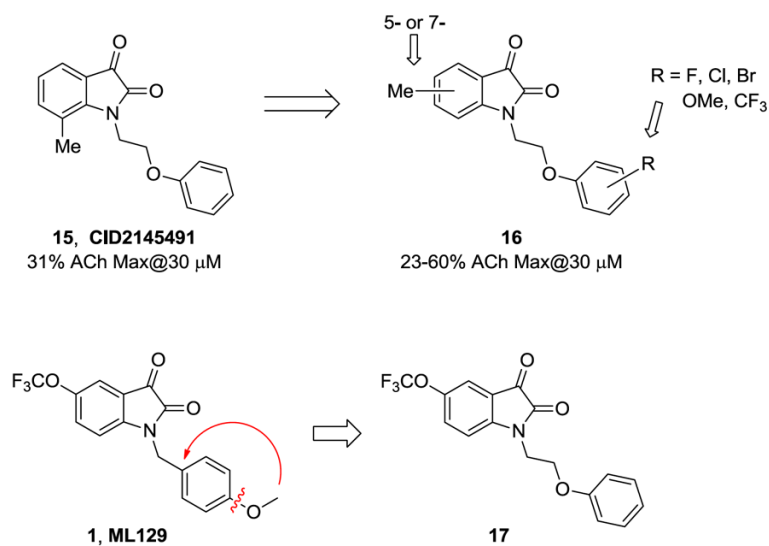


Figure 4.
M₅ Triple-add HTS PAM screening hit **15** and related analogs **16**. Could juxtaposition of ML129 into **17** afford an improved M₅ PAM?

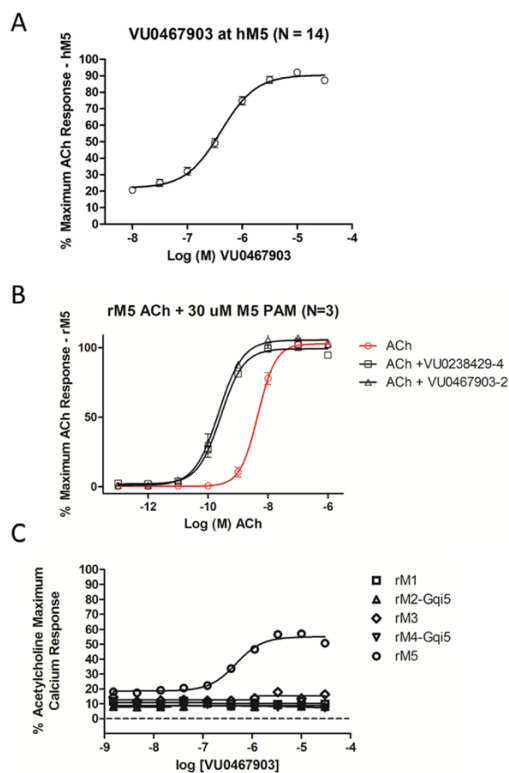
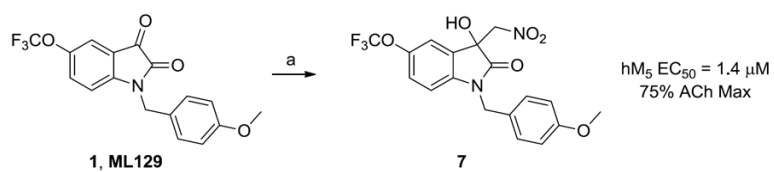
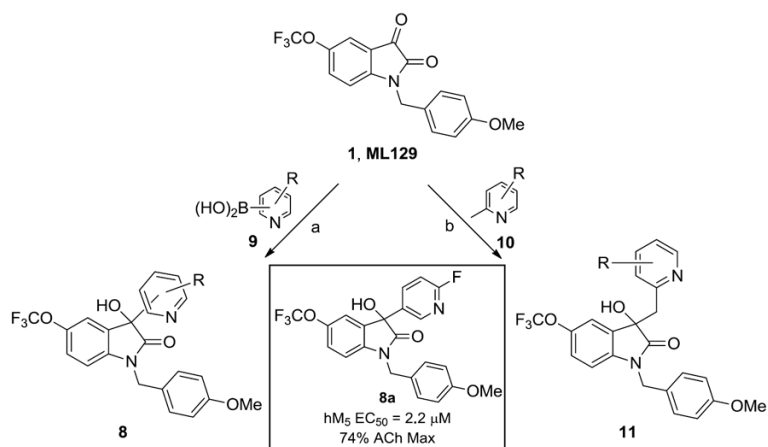


Figure 5.

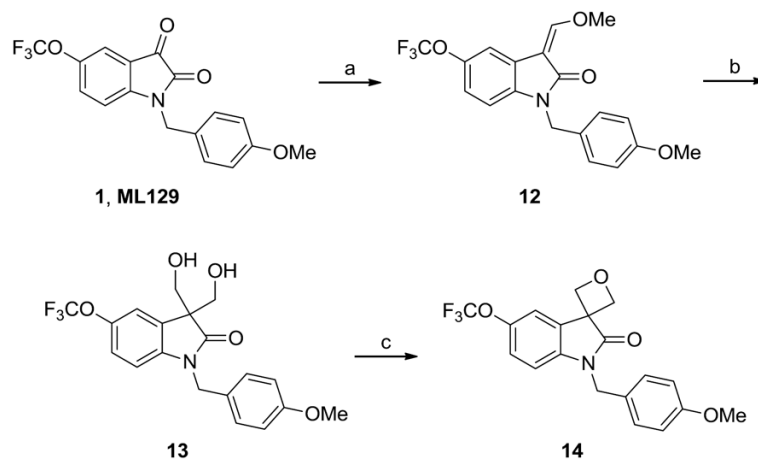
In vitro pharmacological characterization of **17** (VU0467903, ML326). A) M₅ PAM concentration-response-curve (CRC) afforded an EC₅₀ of 409 nM, 91% ACh Max; B) rat M₅ fold-shift assay with **1** (VU0238429, ML129) and **17**, demonstrating a robust 20-fold shift (human fold-shift data is the same). ACh EC₅₀ = 4.58 nM, pEC₅₀ = 8.34±0.04, ACh + 429 EC₅₀ = 263.4 pM, pEC₅₀ = 9.58±0.06, ACh + 903 EC₅₀ = 225.4 pM, pEC₅₀ = 9.65±0.06; C) rat mAChR selectivity data with **17**, indicating >30 μM versus M₁-M₄ (human data is the same).

**Scheme 1.**

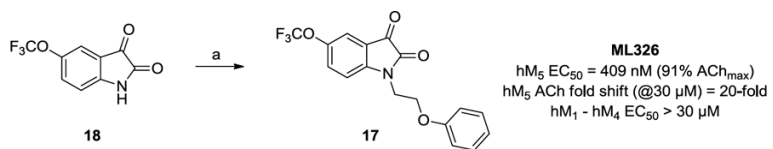
Synthesis of 3° hydroxyl analog **7**. *Reagents and conditions:* (a) DABCO, nitromethane (neat), 100%.

**Scheme 2.**

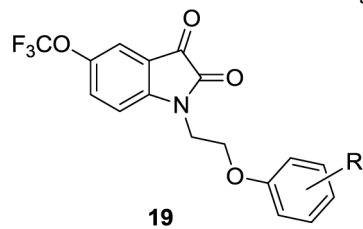
Synthesis of pyridyl-based 3° hydroxyl analogs **8** and **11**. *Reagents and conditions:* (a) Cu(OTf)₂, 1,10-phenanthroline, LiOH, DCE, reflux, 48 hours, 5–45%; (b) TfOH, dioxane, 180 °C, mw, 45 min, 22–74%.

**Scheme 3.**

Synthesis of a spiro-oxetane analog **14**. *Reagents and conditions*: (a) methyl methoxyphosphonium bromide, LDA, THF, -78 °C to rt, 70%; (b) PTSA, aq. formaldehyde, Na₂CO₃, THF:H₂O, rt, 82%; (c) Tf₂O, lutidine, DCM, -78 °C to rt, 6%.

**Scheme 4.**

Synthesis of phenethyl ether analog **17** (**ML326**). *Reagents and conditions:* (a) (2-bromoethoxy)benzene, K₂CO₃, KI, ACN, mw, 160 °C, 10 min, 82%.

Table 1Structures and activities of analogs **19**.

Cmpd	R	M ₅ EC ₅₀ (μM)	pEC50±SEM	%ACh Max
ML326	H	0.41	6.39±0.04	91±1.6
19a	4-OPh	1.05	5.98±0.04	93±1.9
19b	4-Cl	0.45	6.35±0.04	92±1.7
19c	4-OMe	0.59	6.23±0.04	89±1.7
19d	3-Me	0.53	6.28±0.03	91±1.3

All values are the average of three independent experiments.